

DESIGN AND VERIFICATION OF AN INTEGRATED WATER AND FERTILIZER SYSTEM BASED ON IWMA-FUZZY PID REGULATION

基于 IWMA-Fuzzy PID 调控的水肥一体化系统的设计与验证

XiaoYuan ZHU, WeiQiang ZHENG*, LiPing ZHANG

College of Mechanical Engineering, Xinjiang University, Urumqi 830046 / China

Tel: +86-15886154875; E-mail: xjzwwq@xju.edu.cn

DOI: <https://doi.org/10.35633/inmateh-78-95>

Keywords: precision agriculture; nonlinear time-delay system; Improved Whale Migration Algorithm (IWMA); closed-loop control; EC control; dynamic response

ABSTRACT

To address the challenges of nonlinearity, significant time delay, and limited control accuracy in conventional water–fertilizer irrigation systems, this study develops a modular control architecture and proposes a fuzzy PID controller optimized using an Improved Whale Migration Algorithm (IWMA). A hardware platform and a dynamic electrical conductivity (EC) model are established, and real-time closed-loop control is implemented via a programmable logic controller (PLC). Simulation and bench-scale experimental results demonstrate that, compared with conventional PID, fuzzy PID, and PSO-optimized fuzzy PID controllers, the proposed IWMA–fuzzy PID strategy significantly improves dynamic performance. Specifically, the peak time is reduced by 15.2%–56.5%, the settling time by 10.0%–53.0%, and the maximum overshoot is reduced by 0.8%–8.1%. In addition, the proposed method achieves higher steady-state accuracy, faster dynamic response, and enhanced robustness. These results demonstrate the effectiveness and practical applicability of the proposed control strategy in intelligent irrigation systems.

摘要

针对传统水肥灌溉系统存在的非线性、大时滞及控制精度不足等问题, 本文构建了一种模块化控制系统, 并提出一种基于改进鲸鱼迁徙算法 (IWMA) 优化的模糊 PID 控制策略。通过建立硬件平台与电导率 (EC) 动态模型, 并基于可编程逻辑控制器 (PLC) 实现闭环实时控制。仿真与台架试验结果表明, 与常规 PID、模糊 PID 以及 PSO 优化模糊 PID 控制方法相比, 所提出的 IWMA-模糊 PID 控制器在动态性能方面具有显著优势。其中, 峰值时间缩短 15.2%–56.5%, 调节时间缩短 10.0%–53.0%, 最大超调量最高降低 8.1%。同时, 该方法在稳态精度、响应速度及系统鲁棒性等方面展现出更好的综合性能。研究结果表明, 基于 IWMA 的优化方法在智能水肥一体化控制系统中具有良好的工程推广前景。

INTRODUCTION

With the increasingly severe constraints on global population growth and cultivated land resources, the development of precision agriculture is of great significance for safeguarding food security, improving resource utilization efficiency, and promoting the sustainable development of agriculture and the environment. As a key component of precision agriculture, the control level of integrated water and fertilizer application directly affects crop yield, resource utilization efficiency and farmland ecological benefits (Getahun S. et al., 2024). Extensive water and fertilizer management in traditional agricultural production is prone to nutrient loss, triggering problems such as soil degradation and water pollution (Ramoelo A. et al., 2015). Therefore, advancing the transformation of agriculture toward high efficiency and sustainability is in urgent need of the in-depth integration of precision technologies centered on intelligent control (El Bilali H. et al., 2018).

XiaoYuan Zhu, M.S. Stud. Eng.; WeiQiang Zheng, Assoc. Prof. Ph.D. Eng.; LiPing Zhang, Prof. Ph.D. Eng.

Traditional water and fertilizer irrigation systems mostly rely on manual empirical adjustment, which often leads to inaccurate water-fertilizer ratio and increases the risks of fertilizer waste and soil salinization. Meanwhile, the strong nonlinearity, large time delay, and multi-variable coupling characteristics of such systems further increase the difficulty of high-precision control. Although existing studies have achieved certain progress, *Sigrimis et al.*, (2000), designed a greenhouse tomato water and fertilizer system based on the Smith-PID controller, which could control the steady-state error of the EC value within ± 0.2 mS/cm. *Garcia et al.*, (2025), applied fuzzy PID control to the grape drip irrigation system and successfully suppressed the overshoot to approximately 7%. However, these methods still suffer from problems such as over-reliance on empirical parameters and insufficient environmental adaptability (*Sivaraj S.N. et al.*, 2025). Most importantly, previous studies have not fully resolved the contradiction between fast response and small overshoot under strong nonlinear and large time-delay conditions, and the control performance still needs to be improved.

In recent years, the integration of intelligent algorithms with irrigation systems has become an effective approach to improve the control accuracy of water and fertilizer application. Swarm intelligence methods, such as the Grey Wolf Optimizer (GWO) proposed by *Mirjalili et al.* (2014), have been widely applied in PID parameter optimization because of their ability to balance global and local search as well as their good convergence performance (*Singh N. et al.*, 2017). In addition, Particle Swarm Optimization (PSO) and Genetic Algorithm (GA) (*Zhou R. et al.*, 2022; *Dakheel H.S. et al.*, 2023) have also been used for controller parameter tuning. However, in the complex and dynamic environment of water-fertilizer systems, these algorithms still present several limitations, including a tendency to fall into local optima, slow convergence speed, and insufficient population diversity, which make it difficult to meet high-precision real-time control requirements. As a novel swarm intelligence algorithm, the Whale Migration Algorithm (WMA) has shown potential in related fields (*Liu Z. et al.*, 2025). Nevertheless, the original WMA still has certain drawbacks, such as random initialization, redundant leader mechanisms, poor balance between exploration and exploitation, and rigid boundary handling, which restrict its application in high-precision parameter optimization of water and fertilizer systems.

At present, most studies focus on either algorithm improvement or hardware design alone, lacking the deep fusion of modular hardware architecture, dynamic water-fertilizer model, and high-performance intelligent optimization algorithm. The existing optimization algorithms cannot fully adapt to the nonlinear, time-delay, and strongly coupled characteristics of water-fertilizer systems, resulting in limited control accuracy, slow response, and poor robustness.

To fill the above research gaps, this paper proposes an Improved Whale Migration Algorithm (IWMA) to optimize fuzzy PID for water-fertilizer integrated control. Compared with the original WMA and other optimizers, IWMA has four specific improvements: an optimized initialization strategy to improve population quality and convergence speed; an adaptive leader mechanism to enhance guidance efficiency; a dynamic balance between exploration and exploitation to avoid local optima; improved boundary handling to ensure stable and effective iteration.

Based on this, the IWMA algorithm is combined with a modular hardware platform and a dynamic EC model, and closed-loop real-time control is achieved via STM32. Furthermore, simulation and experimental tests are conducted to evaluate the proposed approach against PID, fuzzy PID, and PSO-based fuzzy PID methods. The results demonstrate that the IWMA-fuzzy PID controller exhibits faster dynamic response, reduced overshoot, improved steady-state accuracy, and stronger robustness, indicating its effectiveness for precision water-fertilizer integrated control.

MATERIALS AND METHODS

System Architecture

The core design objective of the integrated water and fertilizer application system is to meet the differentiated demands of crops for water and nutrients (e.g., nitrogen, phosphorus, potassium) at various growth stages.

The system proposed in this study consists of three major modules: the water supply module, the fertilizer suction module and the control module. The water supply module is mainly composed of a water tank, filters and a centrifugal pump. The fertilizer suction module comprises mother liquid tanks for nitrogen, phosphorus and potassium, as well as their supporting components including filters, flowmeters, solenoid valves, pressure gauges, Venturi fertilizer injectors and a fertilizer mixing tank.

The control module is centrally composed of core components such as an EC sensor, a controller and a host computer system. Its specific architecture is shown in Figure 1.

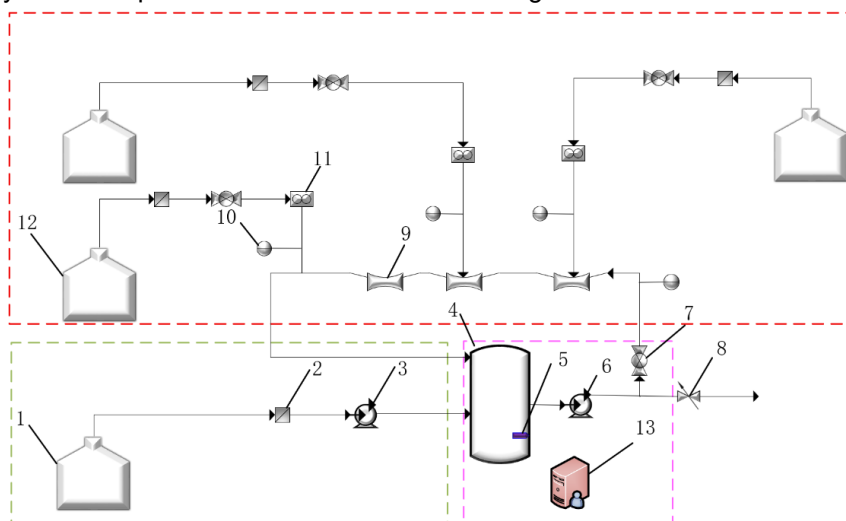


Fig. 1 - Overall Architecture Diagram of the Control System

1 - water tank; 2 - filter; 3 - centrifugal pump; 4 - fertilizer mixing tank; 5 - EC sensor; 6 - fertilizer injection pump; 7 - solenoid valve; 8 - main valve; 9 - Venturi fertilizer injector; 10 - pressure gauge; 11 - flowmeter; 12 - mother liquid tank; 13 - controller and host computer module.

Working Principle

When the system is in operation, the centrifugal pump pumps the filtered irrigation water into the fertilizer mixing tank. The fertilizer injection pump drives the solution in the fertilizer mixing tank through the Venturi fertilizer injector, which generates negative pressure based on the Venturi effect to suck the fertilizer solution from the mother liquid tank into the main irrigation pipeline, thus completing the primary mixing of water and fertilizer. The mixture is then returned to the fertilizer mixing tank for secondary homogenization.

With the STM32 microcontroller serving as the main controller, the system collects real-time data including flow rate, pressure and EC value, and prioritizes monitoring the EC value inside the fertilizer mixing tank, which is further compared with the preset target value. By dynamically adjusting the opening of solenoid valves on each mother liquid branch pipeline, the system can accurately prepare irrigation solution with an EC value that matches the crop growth demand. All operating status and parameters are uploaded to the touch screen host computer in real time, facilitating user monitoring and parameter adjustment.

System Control Model

Model Selection

The EC (electrical conductivity) value is a key parameter that characterizes the total ion concentration of the nutrient solution in integrated water and fertilizer application systems, and its value directly reflects the soluble salt content in the solution. It thus serves as the core basis for the precision regulation of nutrient solutions and the direct control objective of the system proposed in this paper.

There are significant differences in the optimal EC ranges among different crops, and even within the same crop at different growth stages. In addition, EC regulation exhibits strong temporal variability. For example, fruit vegetables such as tomatoes and cucumbers generally require relatively high EC values of 2.0–3.0 mS/cm during the fruiting stage to meet their nutrient demands. In contrast, the optimal EC range for sweet corn throughout the entire growth period is 1.0–2.5 mS/cm, with a lower range of 1.0–1.5 mS/cm recommended during the seedling stage. Similarly, leafy vegetables such as lettuce require EC values to be maintained at 1.0–1.5 mS/cm during the seedling stage to avoid inhibition of growth caused by excessive salinity.

Nutrient Solution Preparation Model Establishment

Precise regulation of the EC value is critical for integrated water and fertilizer application systems. An insufficient EC value indicates a low concentration of available nutrients in the irrigation solution, which will cause nutrient deficiency, slow growth and reduced stress resistance in crops. Conversely, an excessively high EC value reflects an overly concentrated nutrient solution, which can induce osmotic stress and subsequent physiological drought, resulting in leaf scorch, root damage and disruption of the soil microenvironment. This ultimately impairs crop yield and quality while exacerbating the risk of soil salinization. The regulation process of the nutrient solution is illustrated in Figure 2.

Table 1

Nomenclature of Variables and Parameters in Water-Fertilizer Preparation System

Symbol	Physical Meaning	Unit
Q_F	Outlet flow rate of the Venturi fertilizer injector	L/s
Q_M	Flow rate of fertilizer mother liquor	L/s
Q_W	Flow rate of irrigation water flowing into the fertilizer mixing tank	L/s
Q	Outflow rate from the fertilizer mixing tank to the main irrigation pipeline	L/s
Q_0	Flow rate flowing into the Venturi fertilizer injector	L/s
C_W	Concentration of irrigation water	g/L
C_M	Concentration of fertilizer mother liquor	g/L
V_F	Volume of liquid in the Venturi fertilizer injector	L
C_F	Concentration of liquid at the outlet of the Venturi injector	g/L
V_T	Volume of liquid in the fertilizer mixing tank	L
C_T	Concentration of nutrient solution in the mixing tank	g/L
s	Laplace variable	dimensionless
E_1	Electrical conductivity of the irrigation water	mS/cm
$f(t)$	Time-varying control input representing the injection ratio (or valve opening)	dimensionless
τ	System time delay	s
$E_2(t)$	Electrical conductivity of the mixed nutrient solution (system output)	mS/cm
E_m	Electrical conductivity of the fertilizer mother solution	mS/cm

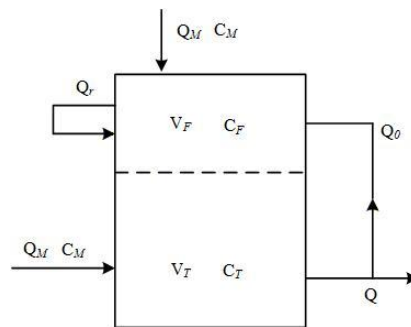


Fig. 2 - Regulation Process of the Nutrient Solution

Q_F - Flow rate of liquid passing through the Venturi fertilizer injector, L/s; Q_M - Flow rate of fertilizer mother liquor, L/s; Q_W - Flow rate of irrigation water flowing into the fertilizer mixing tank, L/s; Q - Flow rate to the main irrigation pipeline, L/s; Q_0 - Flow rate flowing into the Venturi fertilizer injector, L/s; C_W - Concentration of irrigation water, g/L; C_M - Concentration of fertilizer mother liquor, g/L; V_F - Volume of liquid in the Venturi fertilizer injector, L; C_F - Concentration of liquid in the Venturi fertilizer injector, g/L; V_T - Volume of liquid in the fertilizer mixing tank, L; C_T - Concentration of water-fertilizer solution in the fertilizer mixing tank, g/L.

The preparation process of the nutrient solution involves water injection, fertilizer suction, and subsequent mixing in the fertilizer tank. In practice, the fertilizer stock solution is first entrained by the Venturi injector and preliminarily mixed with the irrigation water, and the resulting mixture is then discharged into the fertilizer mixing tank, where further homogenization takes place.

Considering the hydraulic characteristics of the Venturi injector and the fertilizer mixing tank, as well as the dominant dynamic response observed under the experimental operating conditions, the overall nutrient solution preparation process can be approximated by a first-order plus time-delay model. For modeling and analysis, the dynamic characteristics of the process are described based on mass conservation and volume balance.

Based on the principles of mass conservation and volume balance, the dynamic behavior of the nutrient solution preparation process can be formulated. Given the approximately linear relationship between solute concentration and electrical conductivity, the concentration variables are equivalently expressed in terms of conductivity. At dynamic equilibrium, the mass balance of solute concentration can be written as (Carmassi G. et al., 2007; Gallardo M. et al., 2009; Savvas D. et al., 2007; Savvas D. et al., 2008; Varlagas H. et al., 2010):

$$\frac{d[V_F(t)C_F(t + \tau)]}{dt} = Q_0(t)C_T(t) + Q_M(t)C_M - Q_F(t)C_F(t + \tau) \tag{1}$$

These equations describe the concentration and volume dynamics of the mixing process. To facilitate controller design, the concentration variables are further represented by conductivity variables. Similarly, the corresponding volume balance equation is given by:

$$\frac{dV_F(t)}{dt} = Q_0(t) + Q_M(t) - Q_F(t) \tag{2}$$

These equations characterize the dynamic evolution of both solute concentration and liquid volume within the injector system. Considering the approximately linear relationship between solute concentration and electrical conductivity the concentration variables can be equivalently represented by conductivity variables. Specifically, the concentration variables C_W , C_M , and $C_T(t)$ are represented by the conductivity variables E_1 , E_m and $E_2(t)$, respectively.

Furthermore, under steady-state operating conditions, the liquid volume in the fertilizer mixing tank is assumed to remain approximately constant, and the inlet and outlet flow rates are treated as constants during each experiment. Based on these assumptions, the simplified dynamic model can be written as (Meng Z. et al., 2022):

$$Q_W(t)E_1f(t) + Q_M(t)f(t)E_m = V_T \frac{dE_2(t)}{dt} + QE_2(t) \tag{3}$$

Applying the Laplace transform to Equation (3), the transfer function of the system is obtained as (White R.E. et al., 1998):

$$G_s(s) = \frac{E_2(s)}{F(s)} = \frac{Q_W E_1 + Q_M E_m}{V_T s + Q} \tag{4}$$

During the experimental tests, the operating pressure at the equipment outlet was maintained at 0.13 MPa. The measured parameters are as follows:

$$\begin{aligned} V_T &= 30L, q_a = 0.103L/s, q_{100\%} = 0.0518L/s, \\ E_1 &= 0.58mS/cm, E_m = 11.6mS/cm, q_b = 0.8L/s \end{aligned} \tag{5}$$

The system time delay is measured to be 5 s. Substituting these parameters into Equation (4), the transfer function of the EC value in the fertilizer mixing tank can be approximated as:

$$G_s(s) = \frac{0.663}{27.3s + 1} e^{-5s} \tag{6}$$

These results indicate that, although the Venturi injector-tank system involves complex hydraulic and mixing processes, its dominant dynamics can be adequately represented by a first-order plus time-delay model for controller design and performance analysis.

Controller Design

Fuzzy PID Controller

Conventional PID controllers are widely applied in analog control systems due to their advantages of simple structure, stable operation and high reliability. Their control principle is based on the linear combination of proportional (P), integral (I) and derivative (D) operation links for system error, thereby generating the control variable to drive the controlled object (Huang Y. et al., 2000; Chao et al., 2019). However, their parameters usually require pre-tuning; when the system exhibits nonlinear, time-varying and other characteristics, fixed PID parameters may fail to ensure robust control performance (Tang K.S. et al., 2001; Carvajal J. et al., 2000).

For this reason, the fuzzy PID controller integrates the flexibility of fuzzy reasoning with the universality of the PID structure. Through a set of fuzzy rules based on expert experience or a priori knowledge, it dynamically adjusts the PID parameters online according to the real-time system error e and its error rate of change ec , thus constructing a control structure with adaptive capability. Its basic structure is illustrated in Figure 3 below.

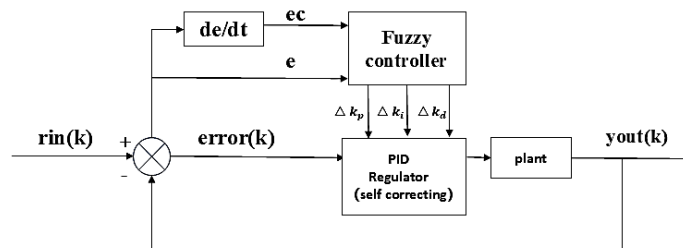


Fig. 3 - Structure Diagram of the Adaptive Fuzzy Controller

The parameter update equations of the fuzzy self-tuning PID controller are given as follows:

$$\begin{cases} K_p = K_{p0} + \Delta K_p \\ K_i = K_{i0} + \Delta K_i \\ K_d = K_{d0} + \Delta K_d \end{cases} \quad (7)$$

where:

K_p , K_i , and K_d denote the proportional, integral, and derivative coefficients after adjustment, respectively; the corresponding initial values are K_{p0} , K_{i0} , and K_{d0} ; ΔK_p , ΔK_i , and ΔK_d represent the respective corrections applied to the proportional, integral, and derivative coefficients.

Controller Optimization

Particle Swarm Optimization Algorithm (PSO)

The PSO algorithm, characterized by simple structure, few parameters, fast convergence, and easy implementation, is well suited for real-time fuzzy PID parameter optimization and engineering applications. Its swarm intelligence mechanism can effectively search for suboptimal parameter combinations. The algorithm simulates the swarm collaborative optimization process: particles update their own states by tracking the personal and global historical optimal positions, and iteratively search for the global optimal solution in the solution space (Wang S. et al., 2022; Yenealem M.G. et al., 2025). The flow chart of the PSO-optimized fuzzy PID controller is shown in the following figure 4.

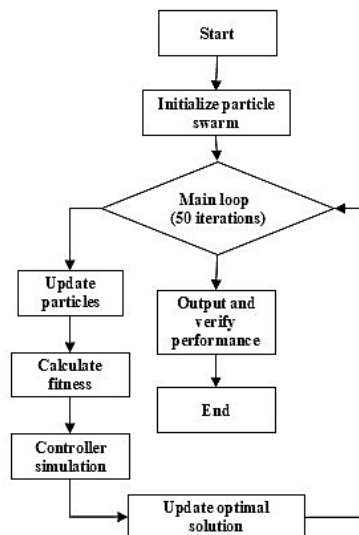


Fig. 4 - Flow Diagram of the Fuzzy PID Controller Optimized by PSO

However, the PSO algorithm is prone to premature convergence accompanied by a rapid decline in particle diversity. Second, it features a relatively single parameter update mechanism and lacks the adaptive adjustment capability based on the search process. Third, it has limited exploration capability for complex coupled parameter spaces, and rigid boundary handling tends to trap particles in local regions. Finally, the absence of a fine search strategy restricts the convergence accuracy in the later stage. Thus, when optimizing the fuzzy PID controller, the PSO algorithm can only obtain local optimal solutions in most cases, making it difficult to achieve the globally optimal parameter configuration (Atyia T. et al., 2025).

Improved Whale Migration Algorithm (WMA)

The Whale Migration Algorithm (WMA) is a swarm intelligence optimization algorithm that simulates the migratory behavior of whale populations in nature, which can efficiently solve complex multi-parameter coupled optimization problems and adapt to the complex and variable agricultural environment. The algorithm performs iterative search via a leader-follower coordination mechanism: individuals with better fitness act as leaders to guide the migration direction, while the remaining followers update their own positions by comprehensively learning the historical information of leaders and the swarm, thus enabling the entire swarm to gradually migrate toward the global optimal solution region. Its core lies in simulating and utilizing the collective intelligence of whale populations characterized by distributed guidance, information sharing and adaptive movement during migration (Ghasemi M. et al., 2025; Ghasemi M. et al., 2024; Lu H. et al., 2025). The flow chart of the Whale Migration Algorithm (WMA) is shown in the following figure 5.

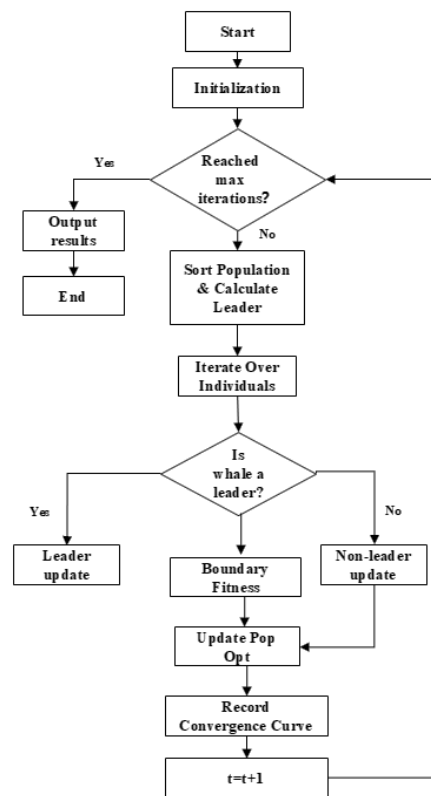


Fig. 5 - Flow Chart of the Whale Migration Algorithm (WMA)

However, the basic Whale Migration Algorithm (WMA) has several inherent flaws in its population initialization and search strategies, which restricts its optimization efficiency and convergence accuracy for solving the fuzzy PID parameter tuning problem of the water-fertilizer EC control system. Specifically, the deficiencies are manifested in four aspects: first, the rough random population initialization strategy may lead to a large number of initial individuals distributed in non-optimal regions, increasing the cost of invalid search; second, the unreasonable setting of the leader proportion is prone to cause redundant information transmission and waste computational resources; third, the rigid boundary handling mechanism is likely to lose potential high-quality solution information; fourth, the lack of elite retention and stagnation mutation mechanisms makes the algorithm vulnerable to falling into local optima and premature convergence.

To overcome the above limitations, this paper improves the WMA algorithm with the following targeted strategies: (1) Initialization Optimization Strategy: An exponential adjustment is adopted using $\text{rand}(\text{VarSize})0.8$, which makes the distribution of initial individuals more concentrated near the parameter boundaries and improves the early exploration efficiency of the algorithm; (2) Leader Streamlining Strategy: The leader proportion is fixed at 15% of the population size ($NL = \text{round}(n\text{Pop} \times 0.15)$) to focus on core information transmission and reduce redundancy. Three key factors are introduced including the global exploration factor α , local exploitation factor δ and adaptive attenuation factor β , which are dynamically adjusted with iteration: a larger α and a smaller δ are set in the early iteration stage to enhance global exploration ability; (3) Adaptive Update and Parameter Regulation Strategy: α is adaptively reduced and δ is increased in the later iteration stage to strengthen local exploitation, thus achieving a dynamic balance between global exploration and local exploitation. Meanwhile, an iteration-decaying perturbation term is added to the individual position update process to prevent premature population aggregation, and the historical optimal solution information is integrated into the update formula to strengthen the algorithm's learning of high-quality solutions.

Algorithm 1: Improved Whale Migration Algorithm (IWMA) for Fuzzy PID Parameter Optimization

Input: Population size N , maximum iterations MaxIter , parameter bounds (LB, UB)

Output: Optimal controller parameters X_{best}

1: Initialize population X_i ($i = 1, 2, \dots, N$) using exponential random distribution

2: Evaluate fitness of X_i and identify initial X_{best}

3: Set leader proportion $NL = \text{round}(0.15 \times N)$

- 4: Initialize adaptive factors α , δ , β
- 5: For $t = 1$ to MaxIter do
- 6: Sort population and select top NL individuals as leaders
- 7: Update α and δ according to iteration t
- 8: For each X_i do
- 9: Update X_i using IWMA rules (leader–follower mechanism with decaying perturbation)
- 10: Apply boundary constraints and evaluate fitness
- 11: End For
- 12: Apply elite retention and stagnation mutation (if no improvement)
- 13: Update X_{best}
- 14: End For
- 15: Return X_{best}

The improved WMA (IWMA) significantly enhances the global search capability, convergence accuracy and anti-premature convergence performance, thus effectively overcoming the inherent flaws of the original algorithm in population initialization, information transmission and boundary handling.

For each input and output variable, seven linguistic terms are introduced within the corresponding fuzzy domain to construct fuzzy subsets. The universe of discourse is defined over the interval $\{-3, 3\}$, where the linguistic values NB, NM, NS, ZO, PS, PM, and PB denote Negative Big, Negative Medium, Negative Small, Zero, Positive Small, Positive Medium, and Positive Big, respectively. Considering system load characteristics and experimental experience, Gaussian membership functions are adopted for the input variables e and ec , while triangular membership functions are selected for the output variables ΔK_p , ΔK_i and ΔK_d . The membership functions are illustrated in Figure 6.

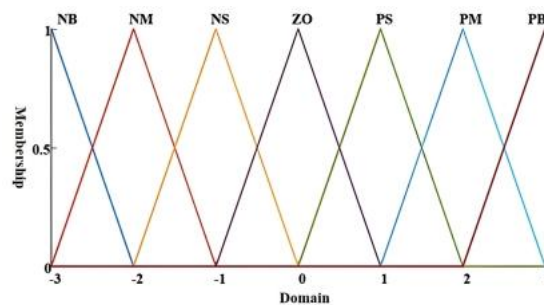


Fig. 6 - Membership Function Diagram

The core of fuzzy PID parameter tuning lies in establishing the fuzzy relationship between ΔK_p , ΔK_i and ΔK_d the system error E and its rate of change EC . The three-dimensional relational surfaces of ΔK_p , ΔK_i , ΔK_d varying with e and ec are shown in Figure 7.

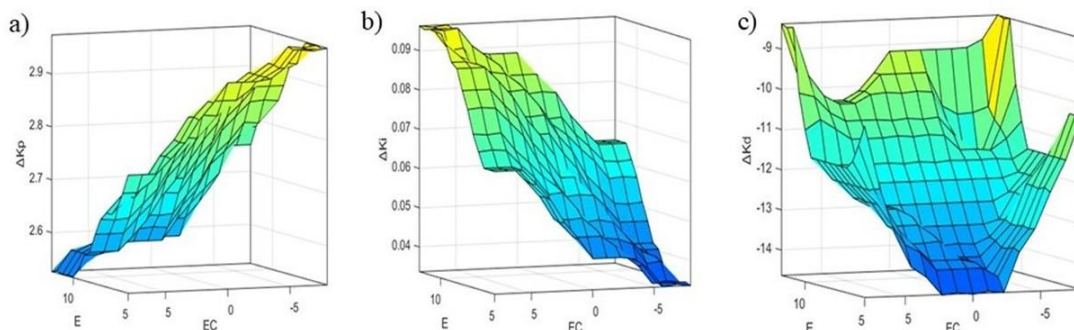


Fig. 7 - Three-Dimensional Variation Diagrams a) 3D Diagram of ΔK_p ; b) 3D Diagram of ΔK_i c) 3D Diagram of ΔK_d

In which the fuzzy control rules for K_p , K_i and K_d are contained in each cell of the table, as shown in Figure 8.

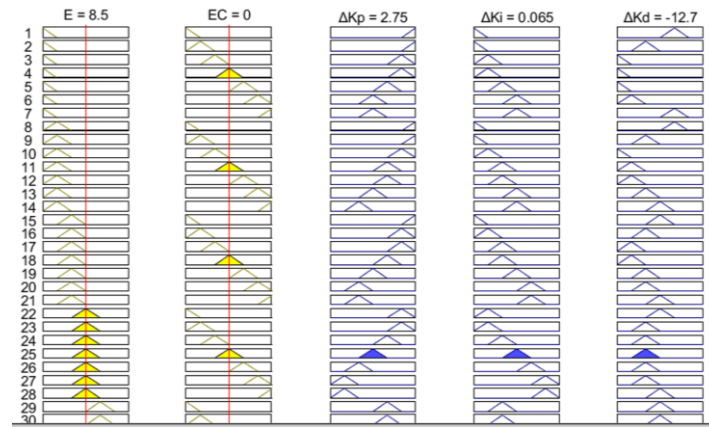


Fig. 8 - Fuzzy Rule Interface

Combining the IWMA with the fuzzy PID controller, the structure of the improved controller is shown in Figure 9.

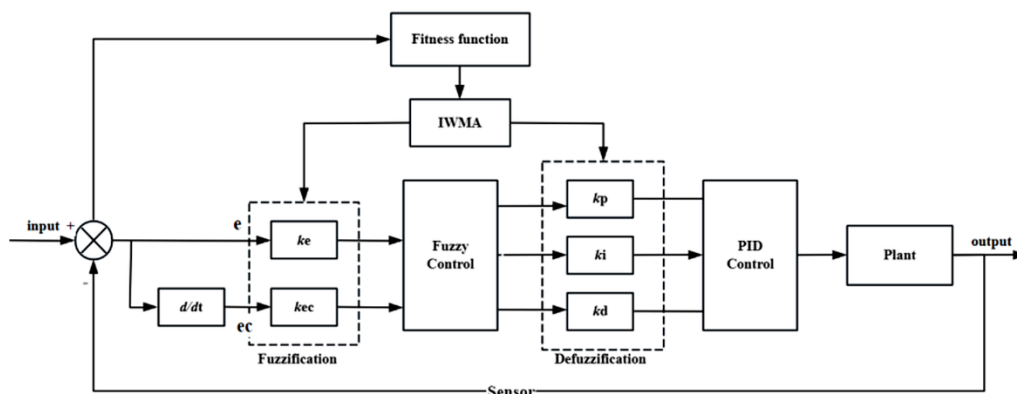


Fig. 9 - Control Principle Structure Diagram

A control simulation model for the EC value of water-fertilizer solution is built based on MATLAB/Simulink R2024a. The total simulation time is set to 300 s, and the system time delay is 5 s. The simulation model includes the established second-order time-delay system model, the fuzzy PID controller module, and the IWMA optimization module, as shown in Figure 10.

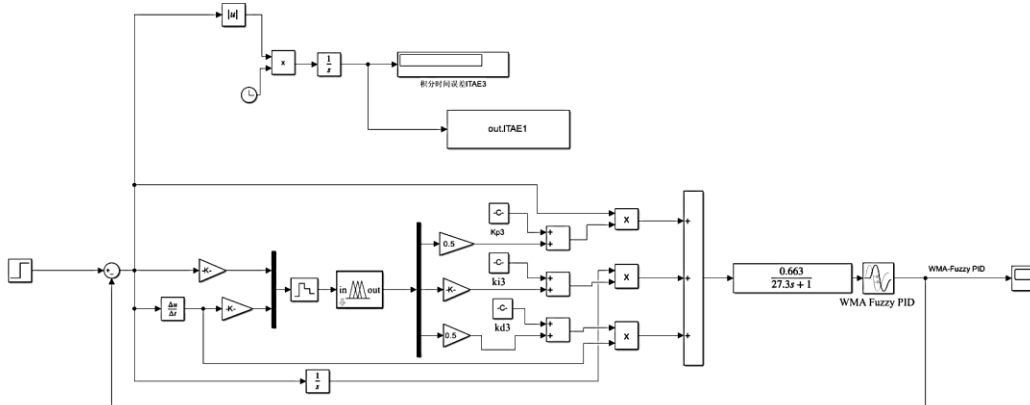


Fig. 10 - Optimization Algorithm Simulation Model Diagram

RESULTS AND ANALYSIS

Simulation Analysis

During the simulation process, comprehensively considering the crop characteristics and system conditions, the target EC value is set to 2.0 mS/cm, with the system sampling period of 0.1 s, system transmission delay of 5 s and simulation duration of 300 s. To ensure the reliability and statistical validity of the simulation results, each control algorithm (Traditional PID, Fuzzy PID, PSO-Fuzzy PID and IWMA-Fuzzy PID) was independently simulated for 30 times under the same system parameters and simulation conditions.

The dynamic performance indices (rise time, peak time, overshoot, settling time) and improvement percentages presented in Table 2 are the average values of the 30 simulation runs, and the standard deviation (SD) is added to reflect the result uncertainty. The comparison results of core dynamic response characteristics are shown in Figure 11 below, and the quantified data of key performance indicators (mean±SD) are presented in Table 2 below.

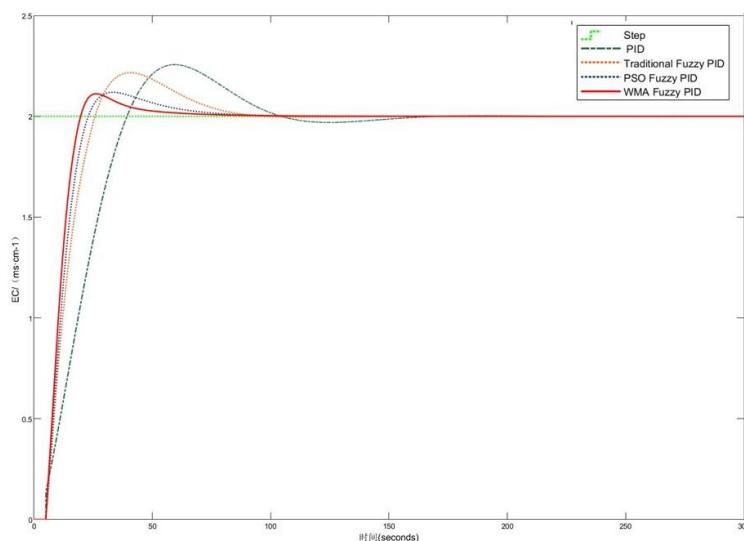


Fig. 11 - Simulation Curve Comparison Diagram of Optimization Algorithm Results

Table 2

Fuzzy Simulation Data Comparison (Mean±SD, n=30)

Control Mode	Rise Time/s	Peak Time/s	Maximum Overshoot	Settling Time/s
PID	27.2±1.32	58.5±2.15	12.85%±0.76%	222.2±8.45
Fuzzy PID	15.2±0.89	39.6±1.78	10.80%±0.52%	152.1±6.32
PSO-Fuzzy PID	12.5±0.67	32.1±1.43	5.95%±0.31%	135.7±5.89
IWMA- Fuzzy PID	10.3±0.45	27.0±1.12	4.85%±0.28%	106.8±4.26

The results indicate that the dynamic performance of the four control algorithms exhibits significant differences, with the IWMA-Fuzzy PID controller achieving the optimal performance. The IWMA-Fuzzy PID controller has a rise time of 10.3±0.45 s, which is reduced by 62.1%, 32.2% and 17.6% compared with the traditional PID (27.2±1.32 s), Fuzzy PID (15.2±0.89 s) and PSO-Fuzzy PID (12.5±0.67 s), respectively; its peak time is 27.0±1.12 s, a reduction of 53.8%, 31.8% and 15.9% in comparison with the above three controllers. This indicates that the IWMA-Fuzzy PID controller can drive the system output to approach the target EC value more rapidly, which effectively improves the dynamic response speed of the system.

Its maximum overshoot is only 4.85%±0.28%, a reduction of 8 percentage points compared with the traditional PID (12.85%±0.76%), 5.95 percentage points lower than the Fuzzy PID (10.80%±0.52%), and 1.1 percentage points lower than the PSO-Fuzzy PID (5.95%±0.31%). This result significantly suppresses the system overshoot phenomenon and reduces the potential impact of severe fluctuations in EC value on crop root systems.

The settling time of the IWMA-Fuzzy PID controller is 106.8±4.26 s, which is reduced by 51.9%, 29.8% and 21.2% compared with the traditional PID (222.2±8.45 s), Fuzzy PID (152.1±6.32 s) and PSO-Fuzzy PID (135.7±5.89 s), respectively. In addition, the fluctuation range of EC value in the steady state is controlled within 0.01 mS/cm, indicating that the IWMA-Fuzzy PID controller can enter the steady state faster and maintain high-precision control of the system.

Error Analysis of Simulation Results

The minor errors in the simulation results (reflected by standard deviation) mainly come from three aspects: first, the randomness of the intelligent optimization algorithm in parameter search, which leads to slight fluctuations in the optimal parameters obtained from each run; second, the small time-delay disturbance of the water-fertilizer EC control system in the actual operation process, which is simplified in the simulation model; third, the quantization error of the sensor data acquisition simulated in the model.

However, the errors are all within a small range (the maximum standard deviation is less than 1.4 s for time indices and 0.8% for overshoot), which has no significant impact on the comparison and analysis of the control performance of each algorithm. In this study, the error is controlled by fixing the random seed in MATLAB and setting the same initial simulation conditions for all algorithms, ensuring the comparability and reliability of the results.

Experimental Verification

Sensor Calibration Procedure

Before the bench-scale test, the core sensors used in the system were calibrated to ensure detection accuracy, especially the EC sensor (KWL-TDS/EC-01, Zhengzhou Kewilai Electronic Technology Co., Ltd.) and flow sensor (K24 turbine flowmeter, Wenzhou Xiaoyao Machinery Co., Ltd.). The calibration process of the EC sensor was as follows: (1) Prepare a series of standard EC solutions with known concentrations (1.0, 1.5, 2.0, 2.5 mS/cm) using analytical grade reagents and deionized water; (2) Immerse the EC sensor probe into the standard solutions in a constant temperature water bath ($25\pm 0.5^\circ\text{C}$) and wait for the reading to stabilize; (3) Record the sensor output value and establish a linear fitting model between the sensor reading and the actual EC value of the standard solution; (4) Correct the sensor detection data using the fitting model during the formal experiment. The calibration accuracy of the EC sensor was controlled within ± 0.05 mS/cm, and the flow sensor was calibrated to an accuracy of ± 0.01 m³/h, which meets the precision requirement of water-fertilizer precision control.

The water supply module of the bench-scale system is mainly composed of water tank 1 and water supply pump 2, which provides water source and power for fertilization and irrigation. The fertilizer suction module mainly consists of nitrogen, phosphorus and potassium fertilizer solution tanks 3, a Venturi fertilizer injector 4 and a fertilizer injection pump 5. The control module is mainly composed of a sensing unit 6 (including the EC sensor KWL-TDS/EC-01 produced by Zhengzhou Kewilai Electronic Technology Co., Ltd.), a host computer 7 and a controller 8 (including the Q941F-16P series solenoid valve manufactured by Shanghai Naite Valve Factory). The sensing unit is used to collect flow rate (the K24 turbine flowmeter produced by Wenzhou Xiaoyao Machinery Co., Ltd.), pressure and EC information, providing decision-making data for water-fertilizer coupling regulation of the system software. The host computer mainly includes a local touch screen and remote user terminal devices. The STM32 single-chip microcomputer is mainly responsible for receiving instructions from the host computer and controlling the switch values of the water-fertilizer irrigation system as well as the rotational speed of the variable-frequency fertilizer injection pump. The specific structure is shown in Fig.12.

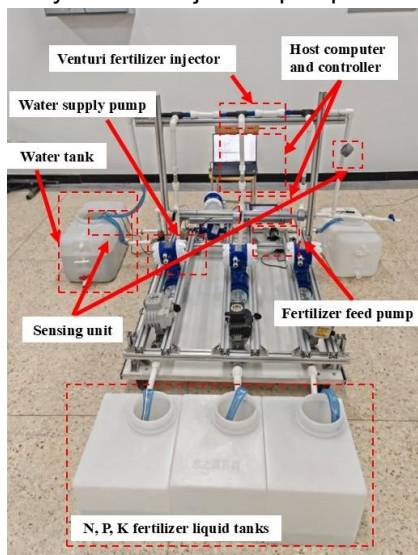


Fig. 12 - Water-Fertilizer Integration Bench-Scale Test Platform

The experimental data are recorded in Table 3, and the bench-scale test results show that: when the target EC values of the system are set to 1.0 mS/cm, 1.5 mS/cm, 2.0 mS/cm and 2.5 mS/cm respectively, the control performance indicators of the IWMA-Fuzzy PID system are superior to those of other algorithms in all aspects. Compared with the traditional PID, its peak time is reduced by 53.1%, 56.5%, 53.3% and 56.0% respectively, the settling time is reduced by 47.6%, 47.0%, 51.7% and 53.0% respectively, and the maximum overshoot is reduced by 7.8%, 7.9%, 8.1% and 8.1% respectively.

Compared with the Fuzzy PID, its peak time is reduced by 40.0%, 35.5%, 33.3% and 37.7% respectively, the settling time is reduced by 23.8%, 25.4%, 30.4% and 29.1% respectively, and the maximum overshoot is reduced by 5.8%, 5.9%, 6.3% and 5.7% respectively.

Compared with the PSO-Fuzzy PID, its peak time is reduced by 25.0%, 23.1%, 15.2% and 17.5% respectively, the settling time is reduced by 10.0%, 13.1%, 19.1% and 19.3% respectively, and the maximum overshoot is reduced by 1.6%, 1.2%, 1.1% and 0.8% respectively.

It can be concluded from the system tests that, compared with the control systems based on the traditional PID, Fuzzy PID and PSO-Fuzzy PID, the control system based on IWMA-Fuzzy PID can adjust the EC value to the vicinity of the set value range more accurately, with a significantly smaller EC value fluctuation range. The system also achieves higher steady-state accuracy, stronger adaptability and better robustness.

Table 3

Fuzzy Simulation Data Comparison

Control Mode	Target EC	Peak Time/s	Settling Time/s	Maximum Overshoot	Steady-State EC mS/cm	EC Fluctuation Range
PID	1.0	32	189	12.7%	0.85~1.12	0.27
	1.5	46	200	12.9%	1.32~1.65	0.33
	2.0	60	228	13%	1.85~2.15	0.30
	2.5	75	249	13.2%	2.37~2.65	0.28
Fuzzy PID	1.0	25	130	10.7%	0.88~1.10	0.22
	1.5	31	142	10.9%	1.35~1.61	0.26
	2.0	42	158	11.2%	1.89~2.12	0.23
	2.5	53	165	10.8%	2.39~2.60	0.21
PSO-Fuzzy PID	1.0	20	110	6.5%	0.91~1.05	0.14
	1.5	26	122	6.2%	1.39~1.58	0.19
	2.0	33	136	6%	1.92~2.10	0.18
	2.5	40	145	5.9%	2.41~2.57	0.16
IWMA-Fuzzy PID	1.0	15	99	4.9%	0.95~1.04	0.09
	1.5	20	106	5%	1.49~1.54	0.05
	2.0	28	110	4.9%	1.94~2.03	0.09
	2.5	33	117	5.1%	2.48~2.56	0.08

CONCLUSIONS

(1) To overcome the limitations of the conventional Whale Migration Algorithm (WMA), this study develops an Improved Whale Migration Algorithm (IWMA) by incorporating enhanced population initialization, an adaptive leader proportion mechanism, and dynamic exploration–exploitation adjustment. These improvements effectively strengthen the global search ability, improve convergence accuracy, and mitigate premature convergence, thereby providing a reliable basis for subsequent controller parameter optimization.

(2) The IWMA-optimized fuzzy PID controller (IWMA-Fuzzy PID) shows superior performance in regulating the EC value of the water–fertilizer mixture. The result of simulation indicate that, compared with conventional PID, fuzzy PID, and PSO-based fuzzy PID controllers, the proposed method shortens response and settling times while reducing overshoot. Consequently, it achieves faster dynamic response, higher steady-state accuracy, and enhanced robustness.

(3) The constructed modular water-fertilizer irrigation control system (consisting of water supply, fertilizer suction and control modules), combined with the proposed IWMA-Fuzzy PID control strategy, performs stably in bench-scale tests with different target EC values (1.0, 1.5, 2.0 and 2.5 mS/cm) with a small EC value fluctuation range. This verifies the feasibility and effectiveness of the integrated design scheme based on the integration of hardware and algorithms in practical applications.

(4) This study applies the intelligent optimization algorithm and advanced control strategy to the water-fertilizer integration system, which provides a high-performance solution for addressing the inherent control challenges of the system such as nonlinearity and strong time delay, and offers a reliable technical reference for the dynamic and precise regulation of water and fertilizer in precision agriculture. However, the current study is limited to bench-scale validation, and further investigation under field conditions is required.

ACKNOWLEDGEMENT

This work was supported by the National Natural Science Foundation of China (52265039) and the Key Scientific Research Project of Xinjiang Uygur Autonomous Region (2022B02028-4).

REFERENCES

- [1] Atyia, T., & Abdullah, S. (2025). Genetic Algorithm of tuning PID for Controlling Speed of DC Motor. *NTU Journal of Renewable Energy*, 9(1), 38-47.
- [2] Chao, C. T., Sutarna, N., Chiou, J. S., & Wang, C. J. (2019). An optimal fuzzy PID controller design based on conventional PID control and nonlinear factors. *Applied Sciences*, 9(6), 1224.
- [3] Carmassi, G., Incrocci, L., Maggini, R., Malorgio, F., Tognoni, F., & Pardossi, A. (2007). An aggregated model for water requirements of greenhouse tomato grown in closed rockwool culture with saline water. *Agricultural water management*, 88(1-3), 73-82.
- [4] Carvajal, J., Chen, G., & Ogmen, H. (2000). Fuzzy PID controller: Design, performance evaluation, and stability analysis. *Information sciences*, 123(3-4), 249-270.
- [5] Dakheel, H. S., Abdullah, Z. B., & Shneen, S. W. (2023). Advanced optimal GA-PID controller for BLDC motor. *Bulletin of Electrical Engineering and Informatics*, 12(4), 2077-2086.
- [6] El Bilali, H., & Allahyari, M. S. (2018). Transition towards sustainability in agriculture and food systems: Role of information and communication technologies. *Information processing in agriculture*, 5(4), 456-464.
- [7] Gallardo, M., Thompson, R. B., Rodríguez, J. S., Rodríguez, F., Fernández, M. D., Sánchez, J. A., & Magán, J. J. (2009). Simulation of transpiration, drainage, N uptake, nitrate leaching, and N uptake concentration in tomato grown in open substrate. *Agricultural Water Management*, 96(12), 1773-1784.
- [8] Garcia, L. D., Lozoya, C., Castañeda, H., & Favela-Contreras, A. (2025). A discrete sliding mode control strategy for precision agriculture irrigation management. *Agricultural Water Management*, 309, 109315.
- [9] Getahun, S., Kefale, H., & Gelaye, Y. (2024). Application of precision agriculture technologies for sustainable crop production and environmental sustainability: A systematic review. *The Scientific World Journal*, 2024(1), 2126734.
- [10] Ghasemi, M., Deriche, M., Trojovský, P., Mansor, Z., Zare, M., Trojovská, E., ... & Kadkhoda Mohammadi, S. (2025). An efficient bio-inspired algorithm based on humpback whale migration for constrained engineering optimization. *Results in Engineering*, 25, 104215.
- [11] Ghasemi, M., Zare, M., Mohammadi, S. K., & Mirjalili, S. (2024). Applications of whale migration algorithm in optimal power flow problems of power systems. In *Handbook of whale optimization algorithm* (pp. 347-364). Academic Press.
- [12] Huang, Y., & Yasunobu, S. (2000, May). A general practical design method for fuzzy PID control from conventional PID control. In *Ninth IEEE International Conference on Fuzzy Systems. FUZZ-IEEE 2000 (Cat. No. 00CH37063)* (Vol. 2, pp. 969-972). IEEE.
- [13] Liu, Z., Li, S., & Xu, H. (2025). An Improved Whale Migration Optimization Algorithm for Cooperative UAV 3D Path Planning. *Biomimetics*, 10(10), 655.
- [14] Lu, H., Cheng, S., & Zhang, X. (2025). An Improved Whale Migration Algorithm for Global Optimization of Collaborative Symmetric Balanced Learning and Cloud Task Scheduling. *Symmetry*, 17(6), 841.
- [15] Meng, Z., Zhang, L., Wang, H., Ma, X., Li, H., & Zhu, F. (2022). Research and design of precision fertilizer application control system based on pso-bp-pid algorithm. *Agriculture*, 12(9), 1395.
- [16] Mirjalili, S., Mirjalili, S. M., & Lewis, A. (2014). Grey wolf optimizer. *Advances in engineering software*, 69, 46-61.
- [17] Ramoelo, A., Cho, M., Mathieu, R., & Skidmore, A. K. (2015). Potential of Sentinel-2 spectral configuration to assess rangeland quality. *Journal of applied remote sensing*, 9(1), 094096-094096.

- [18] Savvas, D., Chatzieustratiou, E., Pervolaraki, G., Gizas, G., & Sigrimis, N. (2008). Modelling Na and Cl concentrations in the recycling nutrient solution of a closed-cycle pepper cultivation. *Biosystems engineering*, 99(2), 282-291.
- [19] Savvas, D., Mantzos, N., Barouchas, P. E., Tsirogiannis, I. L., Olympios, C., & Passam, H. C. (2007). Modelling salt accumulation by a bean crop grown in a closed hydroponic system in relation to water uptake. *Scientia horticulturae*, 111(4), 311-318.
- [20] Sigrimis, N. A., Arvanitis, K. G., & Pasgianos, G. D. (2000). Synergism of high and low level systems for the efficient management of greenhouses. *Computers and electronics in agriculture*, 29(1-2), 21-39.
- [21] Singh, N., & Singh, S. B. (2017). Hybrid algorithm of particle swarm optimization and grey wolf optimizer for improving convergence performance. *Journal of Applied Mathematics*, 2017(1), 2030489.
- [22] Sivaraj, S. N., Vijayakarthick, M., & Vinoth, N. (2025). Criteria maximization for water as well as fertilizer management system using neural network and hybrid PID control. *Scientific Reports*, 15(1), 1-16.
- [23] Tang, K. S., Man, K. F., Chen, G., & Kwong, S. (2001). An optimal fuzzy PID controller. *IEEE transactions on industrial electronics*, 48(4), 757-765.
- [24] Varlagas, H., Savvas, D., Mouzakis, G., Liotsos, C., Karapanos, I., & Sigrimis, N. (2010). Modelling uptake of Na⁺ and Cl⁻ by tomato in closed-cycle cultivation systems as influenced by irrigation water salinity. *Agricultural Water Management*, 97(9), 1242-1250.
- [25] Wang, S., Zhao, B., Yi, S., Zhou, Z., & Zhao, X. (2022). GAPSO-Optimized fuzzy PID controller for electric-driven seeding. *Sensors*, 22(17), 6678.
- [26] White, R. E., Heng, L. K., & Edis, R. B. (1998). Transfer function approaches to modeling solute transport in soils. *Physical Nonequilibrium in soils: modeling and application*, 311-347.
- [27] Yenealem, M. G. (2025). Power flow management and control using PSO-PID and fuzzy logic controllers for autonomous solar and wind hybrid systems. *Cogent Engineering*, 12(1), 2560977.
- [28] Zhou, R., Zhang, L., Fu, C., Wang, H., Meng, Z., Du, C., ... & Bu, H. (2022). Fuzzy neural network pid strategy based on pso optimization for ph control of water and fertilizer integration. *Applied Sciences*, 12(15), 7383.